Computer Physics Communications 48 (1988) 89–96
North-Holland, Amsterdam

AN INTRODUCTION TO SPH

J.J. MONAGHAN

Institute of Astronomy, Cambridge, England
and
Department of Mathematics, Monash University, Clayton, Vict. 3168, Australia

This paper gives the derivation of the equations for SPH (smoothed particle hydrodynamics) and describes their application to a wide variety of problems in compressible gas flow.

1. Preliminary remarks

Smoothed particle hydrodynamics (SPH) was invented to deal with problems in astrophysics involving fluid masses moving arbitrarily in three dimensions in the absence of boundaries. A typical example [1,2] is the numerical simulation of the fission of a rapidly rotating star.

The wide variety of applications of SPH which range from post-Newtonian fluid dynamics to highly supersonic metal and rock collisions (other examples are described by Benz in these proceedings [3]), show that SPH is a versatile tool. There are arguments (see section 9) to suggest that SPH is most effective in three dimensional calculations and least efficient in one dimension, but the full effectiveness of SPH is yet to be determined. After all, finite difference methods have been vigorously studied for forty years by an army of research workers, while SPH has been with us for ten years and its serious study is only beginning.

2. Interpolation from disordered points

SPH involves the motion of a set of points. At any time the velocity and thermal energy are known at these points. A mass is also assigned to each point and, for this reason, the points are referred to as particles. In order to move the particles correctly during a time step it is necessary to construct the forces which an element of fluid would experience. These forces must be constructed from the information carried by the particles.

We begin the task of constructing these forces by considering integral interpolants. Starting with the trivial identity

$$A(\boldsymbol{r}) = \int A(\boldsymbol{r}')\delta(\boldsymbol{r}-\boldsymbol{r}')\,\mathrm{d}\boldsymbol{r}', \tag{2.1}$$

for any field $A(\boldsymbol{r})$, we consider an approximation

$$\langle A(\boldsymbol{r})\rangle = \int A(\boldsymbol{r}')w(\boldsymbol{r}-\boldsymbol{r}', h)\,\mathrm{d}\boldsymbol{r}', \tag{2.2}$$

where $w(\boldsymbol{u}, h)$ is an interpolating kernel with the properties

$$\int w(\boldsymbol{u}, h)\,\mathrm{d}\boldsymbol{u} = 1 \tag{2.3}$$

and

$$w(\boldsymbol{u}, h) \xrightarrow[h\to 0]{} \delta(\boldsymbol{u}).$$

For example, we can choose, in three dimensions

$$w(\boldsymbol{u}, h) = \frac{1}{\pi^{3/2}h^3}\exp(-u^2/h^2), \tag{2.4}$$

although in practice we would usually choose a kernel with compact support. There are infinitely many possible kernels. A discussion of kernels is given in refs. [4–6].

0010-4655/88/$03.50

Suppose now we have a fluid with density $\rho(\boldsymbol{r})$. We can write the RHS of (2.2) as

$$\int [A(\boldsymbol{r}')/\rho(\boldsymbol{r}')]\, w(\boldsymbol{r}-\boldsymbol{r}', h)\rho(\boldsymbol{r}')\, \mathrm{d}\boldsymbol{r}'. \quad (2.5)$$

To evaluate the integral we can imagine the matter divided into N small volume elements with masses $m_1, m_2, \ldots, m_N$. The contribution to the integral from the volume element k with mass m_k and centre of mass $\boldsymbol{r}_k$ is

$$\frac{A(\boldsymbol{r}_k)}{\rho(\boldsymbol{r}_k)} w(\boldsymbol{r}-\boldsymbol{r}_k, h) m_k, \quad (2.6)$$

and an approximation to $\langle A(\boldsymbol{r})\rangle$ is given by

$$\langle A(\boldsymbol{r})\rangle = \sum_{k=1}^{N} m_k \frac{A_k}{\rho_k} w(\boldsymbol{r}-\boldsymbol{r}_k, h) \quad (2.7)$$

where, for example, $A_k := A(\boldsymbol{r}_k)$. When the particles are equi-separated, and their masses are equal, (2.7) is a simple Riemann sum which is equivalent to the trapezoidal rule if A_k/ρ_k vanishes when ρ_k vanishes. In other cases it is more difficult to estimate the accuracy. In the original papers on SPH (2.7) was considered to be a Monte Carlo estimate of (2.2), but it is now clear that this gives much too pessimistic an estimate of the accuracy. A more reasonable estimate is based on the behaviour of quasi-ordered numbers [5] which have an error $\propto (\log_e N)^d/N$ where d is the number of dimensions.

Using (2.7) we can approximate any field A by an analytical function $\langle A(\boldsymbol{r})\rangle$ (if w is n times differentiable then so is $\langle A(\boldsymbol{r})\rangle$). The density estimate is

$$\langle \rho(\boldsymbol{r})\rangle = \sum_{k=1}^{N} m_k w(\boldsymbol{r}-\boldsymbol{r}_k, h), \quad (2.8)$$

which is sometimes interpreted as the smoothing of the particle's point mass by the kernel so as to obtain a continuous density field from a set of particles.

3. Equations of motion

For the present we confine our attention to inviscid fluid dynamics without body forces. To follow the motion of particle i we need an estimate of $\nabla P/\rho$ where P is the pressure. We could calculate this directly, but the symmetrized form obtained from the identity

$$\frac{1}{\rho}\nabla P = \nabla\left(\frac{P}{\rho}\right) + \frac{P}{\rho^2}\nabla\rho, \quad (3.1)$$

leads to exact linear and angular momentum conservation. From (2.7) we find

$$\nabla\left(\frac{P}{\rho}\right) \simeq \nabla\left\langle\frac{P}{\rho}\right\rangle = \sum_{k=1}^{N} m_k \frac{P_k}{\rho_k^2}\nabla w(\boldsymbol{r}-\boldsymbol{r}_k, h), \quad (3.2)$$

and

$$\nabla\rho \simeq \nabla\langle\rho\rangle = \sum_{k=1}^{N} m_k \nabla w(\boldsymbol{r}-\boldsymbol{r}_k, h). \quad (3.3)$$

The momentum equation for particle i can therefore be written

$$\frac{\mathrm{d}\boldsymbol{v}_i}{\mathrm{d}t} = -\sum_k m_k\left(\frac{P_k}{\rho_k^2} + \frac{P_i}{\rho_i^2}\right)\nabla_i w_{ik}, \quad (3.4)$$

where ∇_i means take the gradient with respect to the coordinates of particle i and $w_{ik} := w(\boldsymbol{r}_i - \boldsymbol{r}_k, h)$.

It is worth spending a little time studying (3.4). If w_{ik} is the Gaussian (2.4) then the force per unit mass on particle i due to particle k, F_{ik}, is

$$F_{ik} := m_k\left(\frac{P_k}{\rho_k^2} + \frac{P_i}{\rho_i^2}\right)\frac{2(\boldsymbol{r}_i - \boldsymbol{r}_k)}{h^2} w_{ik}. \quad (3.5)$$

This is a central force and linear and angular momentum are therefore conserved exactly. Although F_{ik} is a pair force it is really a camouflaged many-body force because the coefficient depends on the pressure and density which are determined by the neighbours (see for example (2.8)).

In the absence of heat sources or sinks the rate of change of the thermal energy per unit mass u is given by

$$\frac{\mathrm{d}u}{\mathrm{d}t} = \frac{-P}{\rho}\nabla\cdot\boldsymbol{v}. \quad (3.6)$$

There are several ways this can be written in a

form suitable for computation. For example, start from

$$\frac{P}{\rho}\nabla\cdot v=\frac{P}{\rho^2}\left[\nabla\cdot(\rho v)-v\cdot\nabla\rho\right], \tag{3.7}$$

and use (2.7) to estimate ρv and ρ. Then (3.6) for particle i becomes

$$\frac{\mathrm{d}u_i}{\mathrm{d}t}=\frac{P_i}{\rho_i^2}\sum_{k=1}^{N} m_k(v_i-v_k)\cdot\nabla_i w_{ik}. \tag{3.8}$$

The interpretation of (3.8) is that the thermal energy increases when particles move towards each other (assuming $P>0$, which may be violated for metallic equations of state). We can also use the identity

$$\frac{P}{\rho}\nabla\cdot v=\nabla\cdot\left(\frac{P}{\rho}v\right)-v\cdot\nabla\left(\frac{P}{\rho}\right), \tag{3.9}$$

to deduce the alternative energy equation

$$\frac{\mathrm{d}u_i}{\mathrm{d}t}=\sum_k m_k\frac{P_k}{\rho_k^2}(v_i-v_k)\cdot\nabla_i w_{ik}. \tag{3.10}$$

Experiments with metallic equations of state show that (3.10) results in slightly better energy conservation than (3.8). For ideal gases either form is satisfactory.

Notice that $\mathrm{d}v_i/\mathrm{d}t$ and $\mathrm{d}u_i/\mathrm{d}t$ can only be estimated if ρ is first calculated from (2.8). These summations are lengthy operations, and it is sometimes useful to determine ρ from matter conservation in the form

$$\frac{\mathrm{d}\rho_i}{\mathrm{d}t}=-(\rho\nabla\cdot v)_i=-\sum_k m_k(v_i-v_k)\cdot\nabla_i w_{ik}. \tag{3.11}$$

The right hand sides of (3.4), (3.8) and (3.11) can then be calculated at the same time. By using (3.11) we can eliminate the following difficulty. If we are simulating the impact of two pieces of iron at room temperature and zero pressure, the usual equation of state requires $P=0$ for $\rho=\rho^0$ and $P<0$ for $\rho<\rho^0$. If ρ is estimated from (2.8) we get ρ smoothly falling to zero near the edge and for some particles $\rho<\rho^0$ so there is a local jiggling of the particles driven by the pressure gradient. SPH is trying to simulate the surface and we would prefer it not to! If we use (3.11) we can legislate that for *all* particles, $\rho=\rho^0$ at $t=0$, and the density will only change if particles move towards each other i.e. in the impact.

If the fluid is barytropic, $u=u(\rho)$, and the momentum equation can be obtained from the Lagrangian

$$L=\int\rho\left(\tfrac{1}{2}v^2+u(\rho)\right)\mathrm{d}r, \tag{3.12}$$

which can be approximated by

$$L\sim\sum_k m_k\left(\tfrac{1}{2}v_k^2+u(\rho_k)\right)=:L' \tag{3.13}$$

and eq. (3.4) is obtained from the Lagrangian equations

$$\frac{\mathrm{d}}{\mathrm{d}t}\left(\frac{\partial L'}{\partial v_i}\right)+\frac{\partial L'}{\partial r_i}=0. \tag{3.14}$$

4. Dealing with shocks and penetration

It was found [7] that clouds of gas impacting supersonically were not simulated correctly by the equations described in section 3 because the particles from one cloud penetrated the other and they then streamed through each other. This difficulty was removed by the introduction of an artificial viscosity [8,9]. There are many different possible forms for the artificial viscosity. For example, we can replace (3.4) by

$$\frac{\mathrm{d}v_i}{\mathrm{d}t}=-\sum_k m_k\left[\frac{P_k}{\rho_k^2}+\frac{P_i}{\rho_i^2}+\frac{1}{\bar{\rho}_k k}\left(-\alpha\mu_{ik}\bar{c}_{ik}+\beta\mu_{ik}^2\right)\right]\nabla_i w_{ik}, \tag{4.1}$$

where the notation $\bar{A}_{ik}=\frac{1}{2}(A_i+A_k)$, $A_{ik}=A_i-A_k$, C is the sound speed and if $v_{ik}r_{ik}<0$ (approaching particles)

$$\mu_{ik}=hv_{ik}\cdot r_{ik}/\left(r_{ik}^2+\eta^2\right) \tag{4.2}$$

otherwise $\mu_{ik}=0$. Here η is a clipping function, typically $0.01h^2$. Good results are obtained with $\alpha=1$, $\beta=2$.

It is easy to show that an energy equation consistent with (4.1) is

$$\frac{du_i}{dt} = \tfrac{1}{2}\sum_k m_k \left[\frac{P_i}{\rho_k^2} + \frac{P_i}{\rho_i^2} + \frac{1}{\bar{\rho}_{ik}}\left(-\alpha\mu_{ik}\bar{c}_{ik} + \beta\mu_{ik}^2\right)\right] v_{ik} \cdot \nabla_i w_{ik} \tag{4.3}$$

where the part not involving μ_{ik} comes from half the sum of (3.8) and (3.10).

With these equations excellent results are obtained for shock tube experiments [8] and highly supersonic impacts (isothermal impacts with slightly different artificial viscosity [9] and metal–metal impacts, private communication [3]).

The artificial viscosity has a number of desirable properties. It conserves linear and angular momentum, it is zero for rigid rotation, it is galilean invariant and it produces good shock profiles while stopping penetration. Furthermore, as we will show later, it gives excellent angular momentum transport in astrophysical problems. For many fluid dynamical problems little more is required. However, for sub-sonic flow the dominant linear term leads to a Reynolds number $\sim VL/(hC)$ where the typical velocity $V < C$ and usually $L \sim 20h$ so that the Reynolds number $\lesssim 20/\alpha$ and for reasonable values of α (for these subsonic flows we can take $\alpha \gtrsim 0.1$) the Reynolds number is too low.

It is easy to reduce the artificial viscosity for subsonic flow. For example, in the linear term, the $\bar{C}_{ik}$ can be replaced by

$$\zeta_{ik} := \left(\nu x^2 \mu_{ik} + \mu_{ik}^2 x\right)/\left(\nu x^2 + \mu_{ik}^2\right), \tag{4.4}$$

where $x = \bar{C}_{ik}$ and, from experiments on two dimensional shocks, $\nu \sim 0.1$. If $|\mu_{ik}|$ is sufficiently small $\zeta_{ik} \to \mu_{ik}$ and the artificial viscosity is quadratic in the velocity differences. Unfortunately this also means that sub-sonic streams impinging on each other may penetrate.

The problem of penetration in sub-sonic flow may be solved by following the lead of Brackbill et al. (see these proceedings) and moving the particles with a velocity which differs from the velocity in the momentum equation. For example, we could define a local average velocity difference

$$\Delta v_i = \sum_k \frac{m_k}{\bar{\rho}_{ik}} (v_k - v_i) w_{ik}, \tag{4.5}$$

and write

$$\frac{dr_i}{dt} = v_i + \Delta v_i. \tag{4.6}$$

Linear momentum is conserved (because $\Sigma m_i \dot{r}_i = \Sigma m_i v_i$) and angular momentum is conserved (because $\Sigma m_i v_i \times r_i = 0$) but exact energy conservation is lost (though experiments on mildly supersonic impact show that the errors are small). Ideally we would like Δv_i to vanish for rigid rotation and this can be achieved by inserting the factor $(v_{ki} \cdot r_{ki})^2/(v_{ki}^2 r_{ki}^2)$ into (4.5). It would be interesting to know how effective these devices are for a wide range of problems.

5. Boundaries

In most astrophysical problems boundaries are not important, but in the laboratory they are of the utmost importance. We can distinguish three types of boundary: inflow, outflow and rigid wall. For methods like PIC or FLIP which move particles with a velocity interpolated from the grid the simulation of the boundary presents no more difficulty than for a finite difference scheme. Inflow and outflow boundaries can be described easily by pure particle schemes like SPH though sub-sonic outflow may be more difficult to describe adequately than is the case for finite difference schemes. Rigid walls have been simulated using (a) forces with a length scale h (this mimics the physics behind the boundary condition), (b) perfect reflection and (c) a layer of fixed particles, but there has been no systematic study of boundary simulation with SPH.

6. Implementing SPH

Armed with eqs. (4.1), (4.3) and either (2.8) or (3.11) the problems of galaxy and star formation, binary star interactions, comet and asteroid impacts and self-gravitating disks can be tackled and are in progress.

To implement these problems on a serial machine like the VAX 11/780, link lists provide an effective way of keeping track of those particles

that contribute to a given particle. A calculation of the dynamics of a gas cloud with 4000 particles and a finite difference Poisson solver on a grid $(60)^3$ takes approximately 120 s/time step on a Vax 11/780. The unvectorized program runs 25 times faster on a Cray 1s. The most time consuming sub routines only run about a factor 2 faster when vectorized in the most obvious way to run on the Cray XMP (which has automatic SCATTER and GATHER operations). Duane Marr (Los Alamos, private communication) uses a different logic to get long vectors and achieves a factor 5 over the scalar performance (though the factor depends on the uniformity of the particle distribution in space). For a pure fluid dynamical calculation with 10^6 particles this implies about 2 min per time step. With more supercomputers becoming available, and more of us thinking of 20 h Cray runs as reasonable, it will be possible to study problems such as star formation with the accuracy we know they need.

7. Time stepping

Within the framework of SPH there are many possible forms of time stepping. Early experiments [1,2] used a leap-frog scheme. With the introduction of more complicated physics other schemes have been used. A predictor–corrector method [9] gives good energy conservation while preserving exact linear and angular momentum conservation. Benz (1987) has found the low order Runge–Kutta schemes of Fehlberg to be very efficient.

All the above time stepping schemes are explicit. While no implicit schemes have appeared in the literature the barely implicit scheme of Patnaik et al. [10] could be extended to SPH.

8. Tests of SPH

(a) *Shocks*: Shocktube phenomena involving shock and rare faction waves and contact discontinuities have been simulated by SPH [8,9] for ideal gases. The agreement with theory is excellent and, with high order kernels, the shock thickness is narrow ($\approx 2h$). A wide variety of similar calculations have been made for metallic equations of state (Pongracic and Benz private communication) with good results.

(b) *Dynamics of gas spheres*: The collapse of self-gravitating gas clouds with spherical symmetry has been calculated by SPH and compared with results obtained using a very accurate Lagrangian finite difference scheme. For the isothermal case [6] there is reasonable agreement between the two calculations but working with a resolution length ($\propto h$) which is constant in space precludes an accurate treatment of both the core and the envelope. Evrard [11] uses a resolution which varies in space (see also Wood [12]) and gets good agreement between a 485 particle SPH calculation and a 200 shell Lagrangian calculation of adiabatic collapse. For the expansion of a sphere with initial density $1/r^2$, he finds good agreement with a similarity solution.

These results show that highly non-linear gas dynamics can be modelled efficiently and with reasonable accuracy by SPH.

(c) *Binary star interactions*: The simulation of a system consisting of two self-gravitating stars in orbit about each other creates problems for many finite difference schemes. There is a lot of empty space and the gas convects matter and angular momentum through the grid. Errors show up in the gas moving away from the correct orbit (spiralling in or out). SPH always gives good results for these problems. It predicts instabilities correctly and follows the motion produced by tidal forces accurately [13].

(d) *Angular momentum transport*: The binary star problem already shows that SPH can give good angular momentum transport. The collapse of a rotating gas cloud [7,6] shows that even with the density changing during the calculation by two orders of magnitude vorticity is conserved satisfactorily. The errors that do occur are probably due to the finite difference calculation of gravity since, in a two dimensional collapse in a potential r^2, the change in the vorticity invariant < one percent up to the first bounce. These calculations involve supersonic motion. If the motion is subsonic (see (e)) the low Reynolds number mentioned earlier (section 4) informs us that the transfer of angular momentum will be inaccurate and sometimes badly wrong.

(e) *A shear instability*: A problem which has gained some notoriety is the evolution of a fluid which, at $t = 0$, is at rest except for a cylinder of fluid which rotates rigidly. At the interface between the non-rotating and rotating fluid a shear instability develops. This is not a good test problem because the true evolution is unknown but we can compare the results of different numerical methods. In fig. 1 the evolution of a system which at $t = 0$ has speed of sound = 1, angular velocity Ω of the unperturbed inner cylinder = $1/2$ and radius of the inner cylinder = 1, is shown. For this case there are 256 particles in the inner cylindrical region which is defined by $r \leqslant 1 + 0.1 \cos 4\theta$ and in this region $v_r = 0$, $v_\theta = r\Omega$. The parameters of the artificial viscosity are $\alpha = 0.1$, $\beta = 0$. The system evolves as expected producing four vortices, but the detail is not as fine as in the simulation using FLIP. In this problem FLIP has the advantage that for a given scale of instability, adequately resolved by the grid, more and more particles can be placed in the cells with little extra cost, but greatly improved definition of the interface. An SPH calculation with similar definition would involve a much longer calculation. Note that the motion in this problem is subsonic and the Reynolds number in the SPH calculation is ~ 50.

(f) *Viscous diffusion of a ring*: The evolution of viscous disks and rings is an important process in astronomy. When the fluid in the disk can be treated as cold (negligible pressure), two dimensional, adiabatic and moving in the gravitational

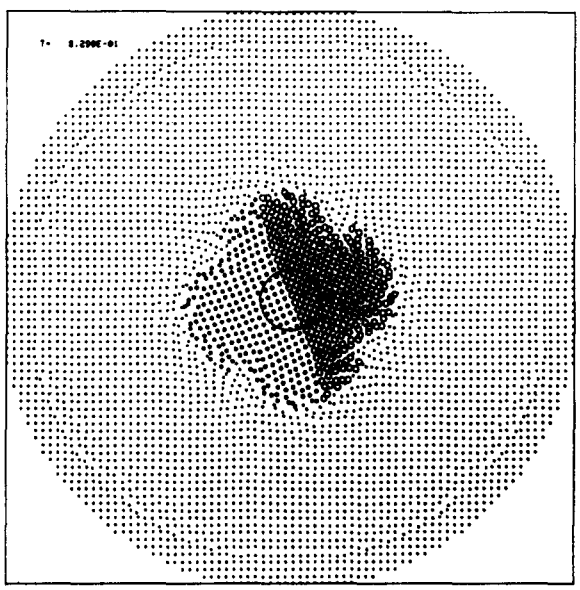

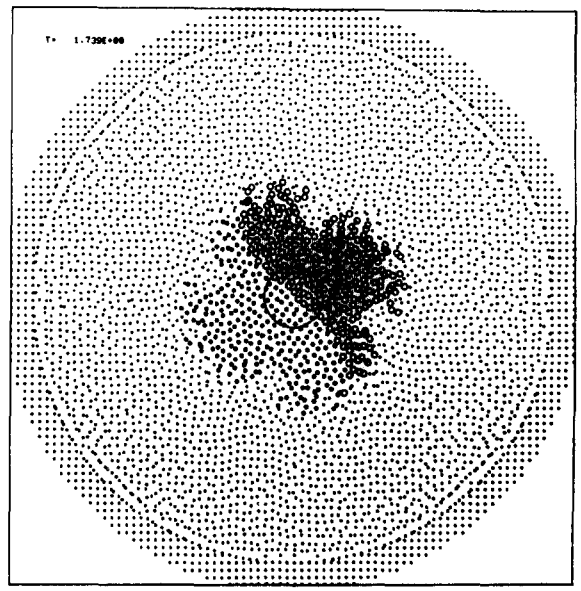

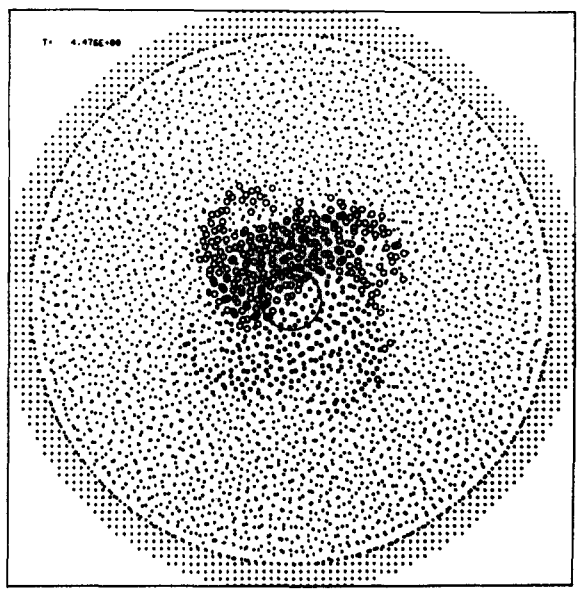

Fig. 1. The evolution of a two-dimensional compressible gas. At $t = 0$, $v = 0$ unless $r < (1 + 0.1 \cos 4\theta)$ when $v = \Omega \times r$ and $\Omega = 0.5$. The artificial viscosity parameters are $\alpha = 0.1$, $\beta = 0$. Different particle symbols are used to help indicate the motion. The central circle has radius = $2h$.

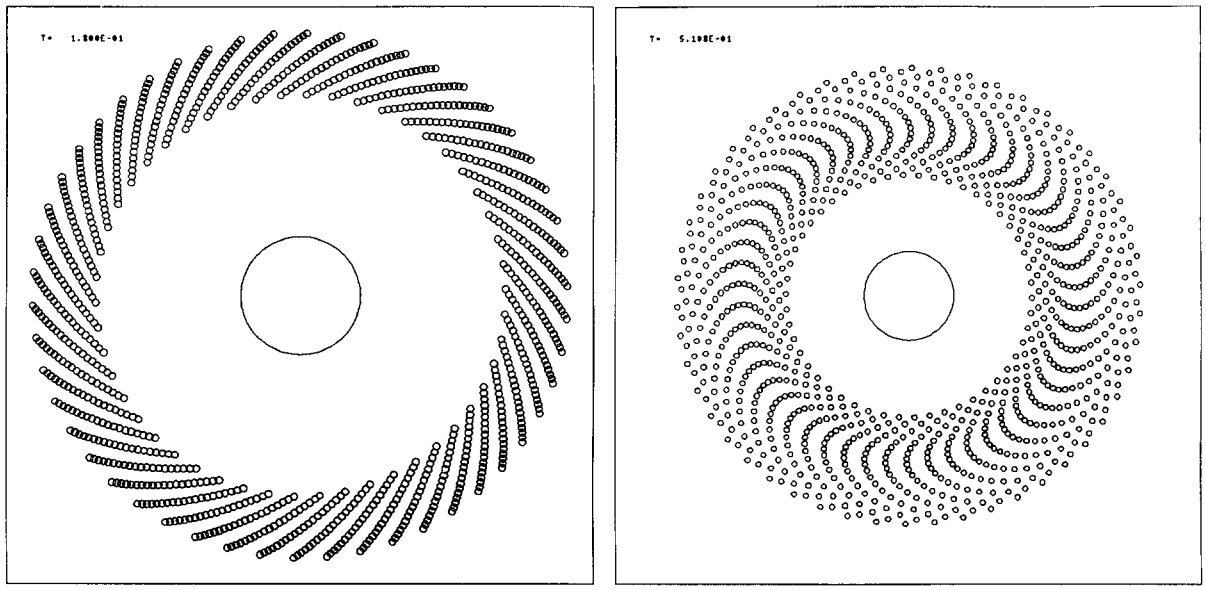

Fig. 2. The evolution of a cold viscous ring with $\alpha = 1.0$ and $\beta = 0$. The central circle has radius $= 2h$. Angular momentum is conserved exactly and the axial symmetry is maintained.

field of a point mass, the equations of motion reduce to a single linear partial differential equation [14]. When the initial density is a delta function in radius an exact solution can be found.

We simulate the diffusion of such a ring by starting with the density $r = \exp((r - r_0)^2/l^2)$ with $l \ll r_0$. A typical example of a simulation is shown in fig. 2 where we have chosen artificial viscosity parameters $\alpha = 1.0$, $\beta = 0$ and taken speed of sound 1.0 in the artificial viscosity formula. The mass of the central object is such that the initial equilibrium velocity is Mach 7 at $r = r_0$. All particles are given a velocity which would produce equilibrium in the absence of viscosity.

The SPH results are in excellent agreement with the analytical results. Furthermore the initial symmetry is maintained and angular momentum is conserved exactly. Simulations with $\alpha = 9$ and $\alpha = 0.1$ also give excellent agreement with theory.

(g) *Magnetohydrodynamics*: Phillips and Monaghan [15] have simulated Alfvén waves and static MHD gas clouds and found good agreement with theory.

9. Comments on accuracy and resolution

The accuracy of the integral interpolant (2.2) depends on the form of the kernel. Taylor series expansion of the integrand about r shows that the dominant error term, if W is an even function, is $h^2(\nabla^2 A)$. If the kernel is chosen so that

$$\int u^2 w(\boldsymbol{u}, h)\, \mathrm{d}\boldsymbol{u} = 0,$$

the error is $\mathcal{O}(h^4)$. However, these kernels do not satisfy $W \geqslant 0$ and they should be used with caution (see Lattanzio et al. [9]). Replacing the integral interpolant by the sum (2.7) introduces further errors. If, as suggested the points are quasi-ordered, these errors are $\mathcal{O}((\log_e N)^d/N)$ or equivalent $\mathcal{O}((h \log_e h)^d)$ where d is the number of dimensions and we assume here $N \propto 1/h^d$. In one dimension the integration errors dominate and we expect errors of $\mathcal{O}(h \log h)$ while in three dimensions the errors in the interpolant (assumed $\mathcal{O}(h^2)$) dominate. We infer low accuracy in one dimension and competitive accuracy in three di-

mensions. Of course for many problems, the shock tube experiments are an example, the particles in one dimension are highly ordered and the error estimates made above are overly pessimistic.

Most astrophysical calculations have used an h which varies in time according to $h \propto 1/(\bar{\rho})^{1/d}$ where $\bar{\rho}$ is the average density. It would clearly be an advantage to have h vary in space. Calculations with an h for each particle have been performed [12,16,11] with satisfactory results. However, no systematic study of different formulations of the spatially variable h form of SPH have appeared in the literature.

10. Summary

SPH has been used and tested on many highly non-linear problems. It is simple to program (a typical 3D program involves only 900 lines of code) and, like other particle methods, is very robust. It would be desirable to explore, systematically, techniques for introducing a spatially varying resolution length since this would open up a number of difficult problems to attack. Other areas where more work is needed are the treatment of rigid boundaries and the use of local averaged velocities to move particles.

References

[1] R.A. Gingold and J.J. Monaghan, Mon. Not. Roy. Astr. Soc. 181 (1977) 375.
[2] L.B. Lucy, Astron. J. 82 (1977) 1013.
[3] W. Benz, Los Alamos National Laboratory, private communication.
[4] J.J. Monaghan, SIAM J. Sci. Stat. Comput. 3 (1982) 422.
[5] J.J. Monaghan, Comput. Phys. Rep. 3 (1985) 71.
[6] J.J. Monaghan and J.C. Lattanzio, Astron. Astrophys. 149 (1985) 135.
[7] R.A. Gingold and J.J. Monaghan, Mon. Not. Roy. Astr. Soc. 204 (1983) 715.
[8] J.J. Monaghan and R.A. Gingold, J. Comput. Phys. 52 (1983) 375.
[9] J.C. Lattanzio, J.J. Monaghan, H. Pongracic and M.P. Schwarz, SIAM J. Sci. Stat. Comput. 7 (1986) 591.
[10] G. Patnaik, R.H. Guirgius, J.P. Boris and E.S. Oran, J. Comput. Phys. 71 (1987) 1.
[11] A.E. Avrard, preprint P3MSPH – A Numerical Tool for 3-D Cosmological Gas Dynamics, Inst. of Astronomy, Cambridge, England (1987).
[12] D. Wood, Mon. Not. Roy. Astr. Soc. 194 (1981) 201.
[13] R.A. Gingold and J.J. Monaghan, Mon. Not. Roy. Astr. Soc. 191 (1980) 897.
[14] J.E. Pringle, Ann. Rev. Astron. Astrophys. 19 (1981) 137.
[15] G.J. Phillips and J.J. Monaghan, Mon. Not. Roy. Astr. Soc. 216 (1985) 883.
[16] M. Loewenstein and W.G. Mathews, J. Comput. Phys. 62 (1986) 414.